

Abstract: A search is underway to find baryon resonances that have been predicted, but yet remain unobserved. Nucleon resonances, due to their broad energy widths, overlap and must be disentangled in order to be identified. Meson photoproduction observables related to the orientation of the spin of the incoming photon and the spin of the target proton are useful tools to deconvolute the nucleon resonance spectrum. These observables are particularly sensitive to interference between phases of the complex amplitudes. A set of these observables has been measured using the CEBAF Large Acceptance Spectrometer (CLAS) at Jefferson Lab with linearly-polarized photons having energies from 725 to 2100 MeV with polar angle values of $\cos(\theta_{C.M.})$ between -0.8 and 1 and transversely-polarized protons in the Jefferson Lab FROZEN Spin Target (FROST). By fitting neutron yields over azimuthal scattering angle, the observables H and P have been extracted. Preliminary results for these observables will be presented and compared with predictions provided by the SAID Partial-Wave Analysis Facility.

Motivation

When a high-energy photon impinges on a nucleon, the nucleon is excited into a new state. This state is called a resonance, and it leads to the creation of new baryons and mesons that depend on the energy of the resonance. Predicted nucleon resonances, due to the uncertainty principle, have an inherent width that is inversely proportional to their lifetime. As a result, many resonances overlap, as can be seen at right (Figure 1) for the reaction $\gamma p \rightarrow \pi^+ n$. In order to better understand the excitation of nucleons, these resonant states must be deconvolved so that competing models for explanation of these states can be compared. One way of achieving this is by exploiting the interference between the phases of the complex amplitudes of the wavefunctions involved. To exploit this property, differing polarizations of both the target proton and the incoming photon can be used to cause interference that helps to reveal different underlying resonances.

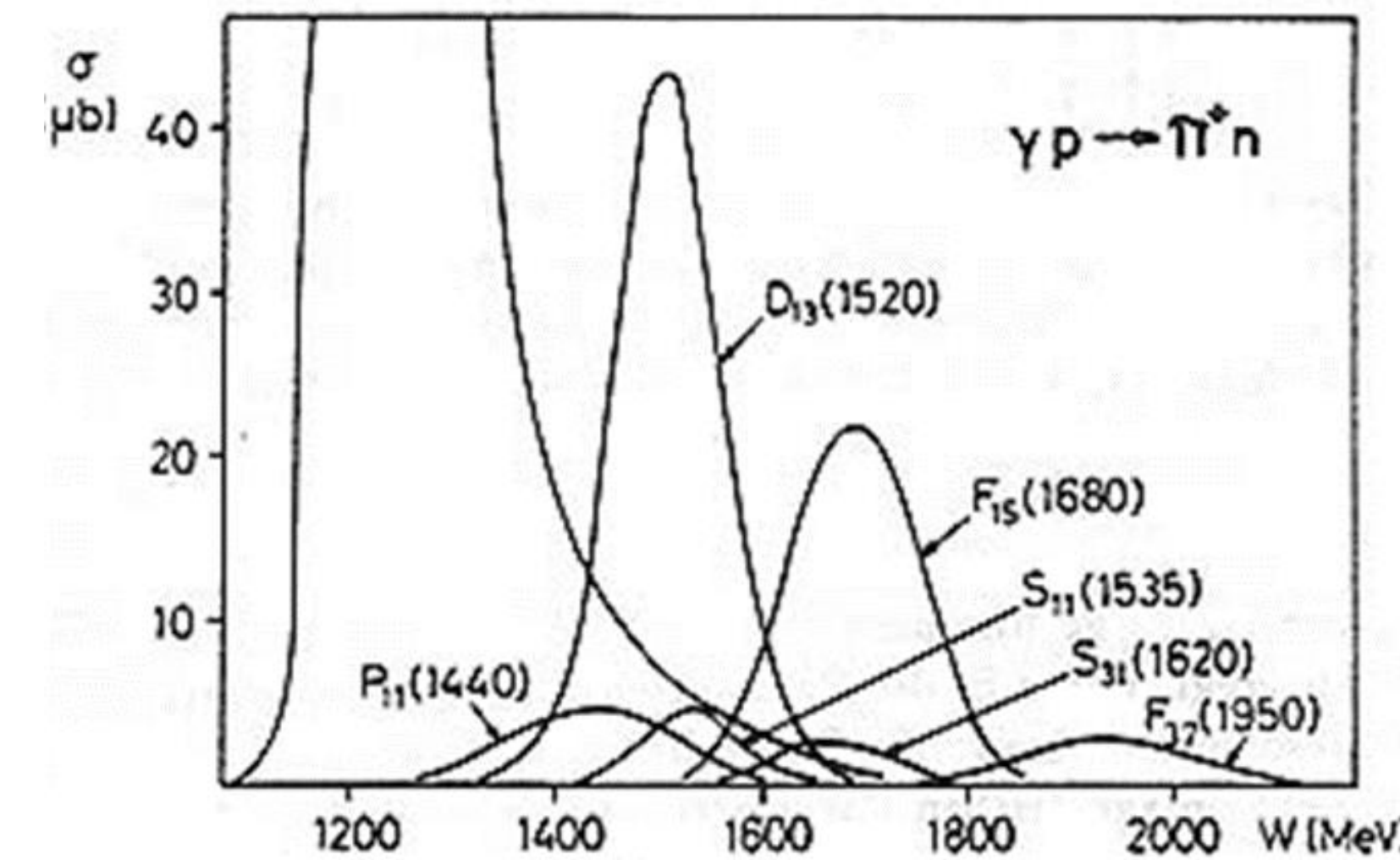


Figure 1: Plot showing overlapping baryon resonances

Experimental Facility

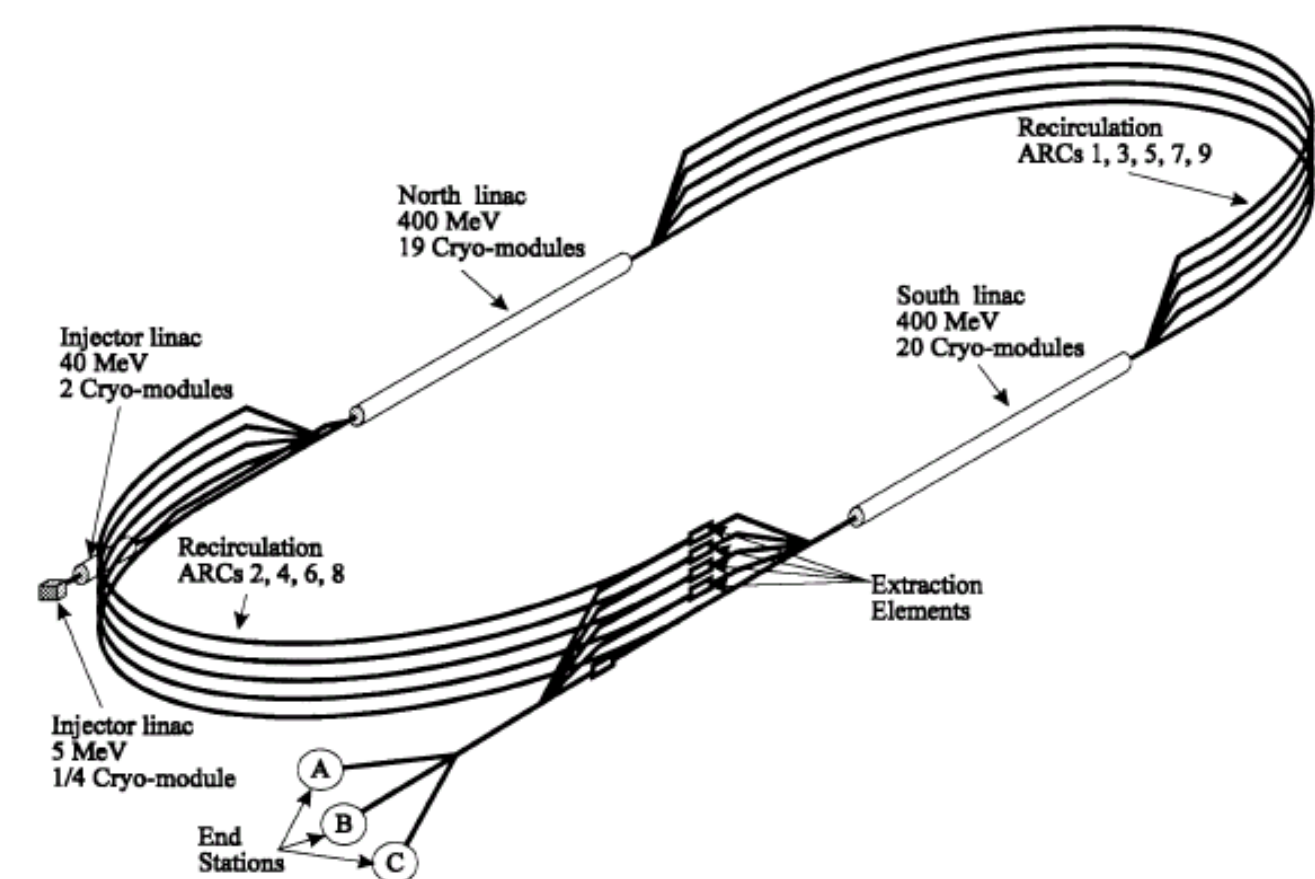


Figure 2: Sketch of the Continuous Electron Beam Accelerator Facility (CEBAF)

Data were obtained from Hall B of Jefferson National Laboratory's Continuous Electron Beam Accelerator Facility (CEBAF). A sketch of CEBAF can be seen at left in Figure 2. This facility uses high-energy electron beam photoproduction to produce photons of various controlled energies. These photons are then incident on the Frozen Spin Target (FROST) within the CLAS detector contained in hall B.

The FROST target consists primarily of butanol ($C_4H_{10}O$), which has an abundance of hydrogen, and therefore is proton-rich. Using a magnetic field (0.5T) and very low temperatures ($\sim 0.5K$) in order to minimize random thermal motion, a strong polarization of the target protons can be maintained.

The reaction products that result from the collision of the polarized photons with the polarized protons are then detected by the CEBAF Large Acceptance Spectrometer (CLAS), which can be seen to the left (Figure 3). By applying a strong magnetic field and using various detector elements, particle masses and energies can be determined and the resulting particles can therefore be identified based on their path through CLAS.

Knowledge of the incoming photon polarizations and energies can then be combined with information about the outgoing momenta and spatial distributions to perform detailed analysis on polarization observables of the interaction, as will be discussed in the Analysis Methods section.

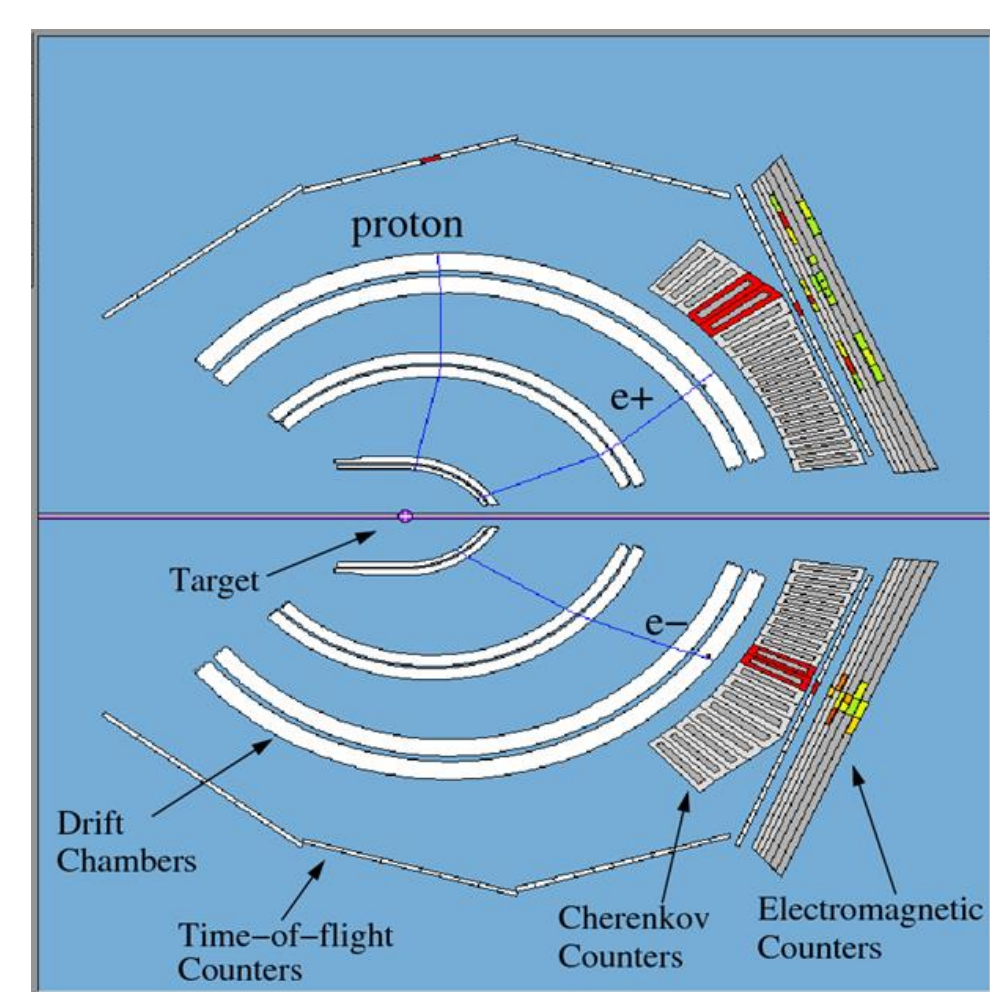


Figure 3: Sketch of the CEBAF Large Acceptance Spectrometer (CLAS)

Analysis Methods

From quantum-mechanical calculations, the dependence of the differential cross section on polarization, azimuthal angle, and various other observable quantities can be constructed. For a linearly-polarized photon beam and transversely-polarized target, the following equation represents the differential cross section

$$\frac{d\sigma}{d\Omega} = \frac{d\sigma_0}{d\Omega} (1 - P_T \Sigma \cos(2\phi) + P_{XY}^{Lab} P_T H \cos(\beta - \phi) \sin(\phi) + P_{XY}^{Lab} T \sin(\beta - \phi) - P_{XY}^{Lab} P_T P \sin(\beta - \phi) \cos(2\phi)), \quad (1)$$

where $\frac{d\sigma_0}{d\Omega}$ is the differential cross section without polarization, P_T the polarization value for the photons, P_{XY}^{Lab} the polarization value for the target, β the offset angle between the polarization of the target and beam, ϕ is the azimuthal angular location of the outgoing π^+ and the quantities P and H are the observables that are to be measured by this analysis.

The differential cross section can be analyzed in terms of the yields of particles at various angles, as the cross section can be thought of as a likelihood of interaction. By using different values of P_{XY}^{Lab} and P_T , the yields can be combined carefully to isolate only the desired observables, H and P . Ignoring numerical prefactors, the general form of this combination is

$$H \cos(\beta - \phi) \sin(2\phi) - P \sin(\beta - \phi) \cos(2\phi) \propto \frac{(Y_{++} + Y_{--}) - (Y_{+-} + Y_{-+})}{(Y_{++} + Y_{--}) + (Y_{+-} + Y_{-+})} \quad (2)$$

Where Y represents the value of the yield, and the subscripts + and - represent the directions of the target and photon polarization.

In order to properly extract the H and P observables, the yields of neutrons must be carefully measured to make sure that the reaction of interest was, in fact, observed. To extract the neutron, a missing mass plot can be constructed after the various events are combined as shown in equation 2. Since there is generally a background of undesired outgoing particles, the neutron peak must be isolated, and the background removed in the integration of total yield. An example of the fitting can be seen below in Figures 4 (numerator) and 5 (denominator), where the plot corresponds to the yield in a single azimuthal sector of the detector.

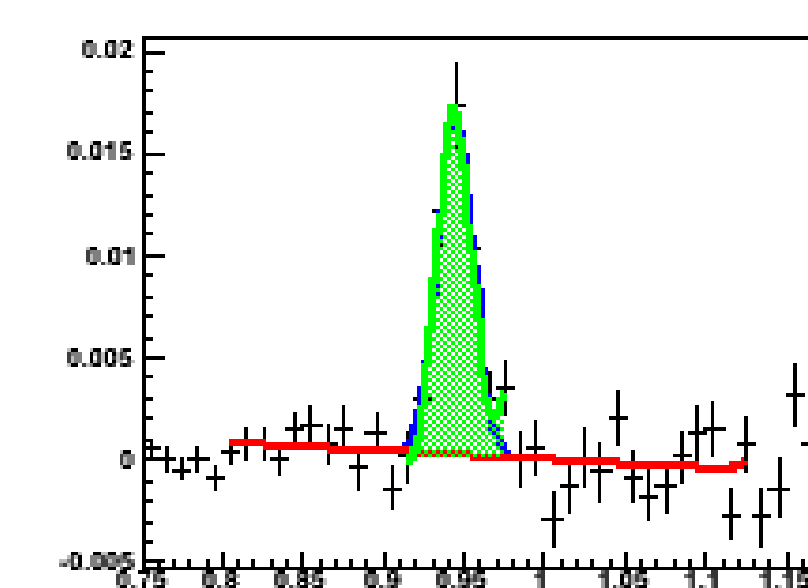


Figure 4: Plot showing integration of yields for the numerator

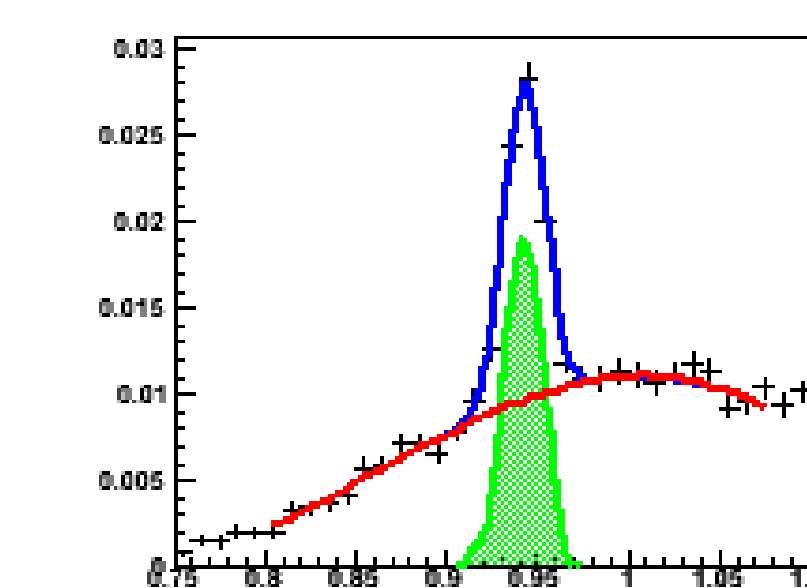


Figure 5: Plot showing integration of yields for the denominator

The azimuthal yields can then be plotted as a function of the angle, as shown to the right in Figure 6. Here, each of the points corresponds to the division of the numerator by the denominator for a specific sector and binned in terms of azimuthal angle. The resulting azimuthal distributions are fit by the left hand side of equation 1. From the fit, the values for the observables H and P are extracted. The only step that then remains is to plot these values of H and P as a function of the cosine of the polar angle in the center-of-mass frame. Plots of H and P are obtained for various incoming photon energies (between 725 MeV and 2100 MeV in 50 MeV increments), and are compared to theoretical predictions from the SAID Partial Wave Analysis Facility.

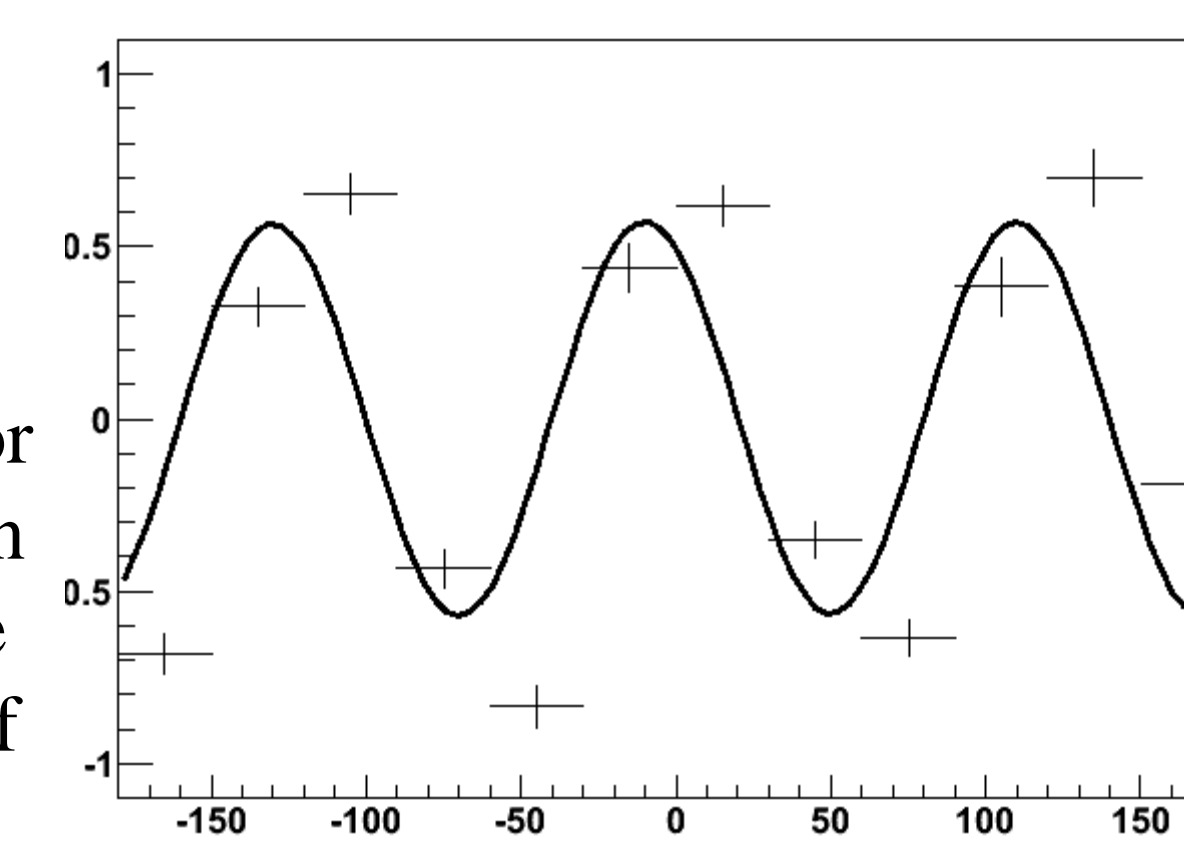


Figure 6: Example fit of yields distributed in azimuthal angle to equation given above

Results for H and P

Below, preliminary results for H (Left) and P (Right) are compared to predictions for the observables generated by the SAID Partial Wave Analysis. The predictions correspond to the SM95 solution (Red) and the PR15 solution (Blue), where the changes are due to new data for a different reaction

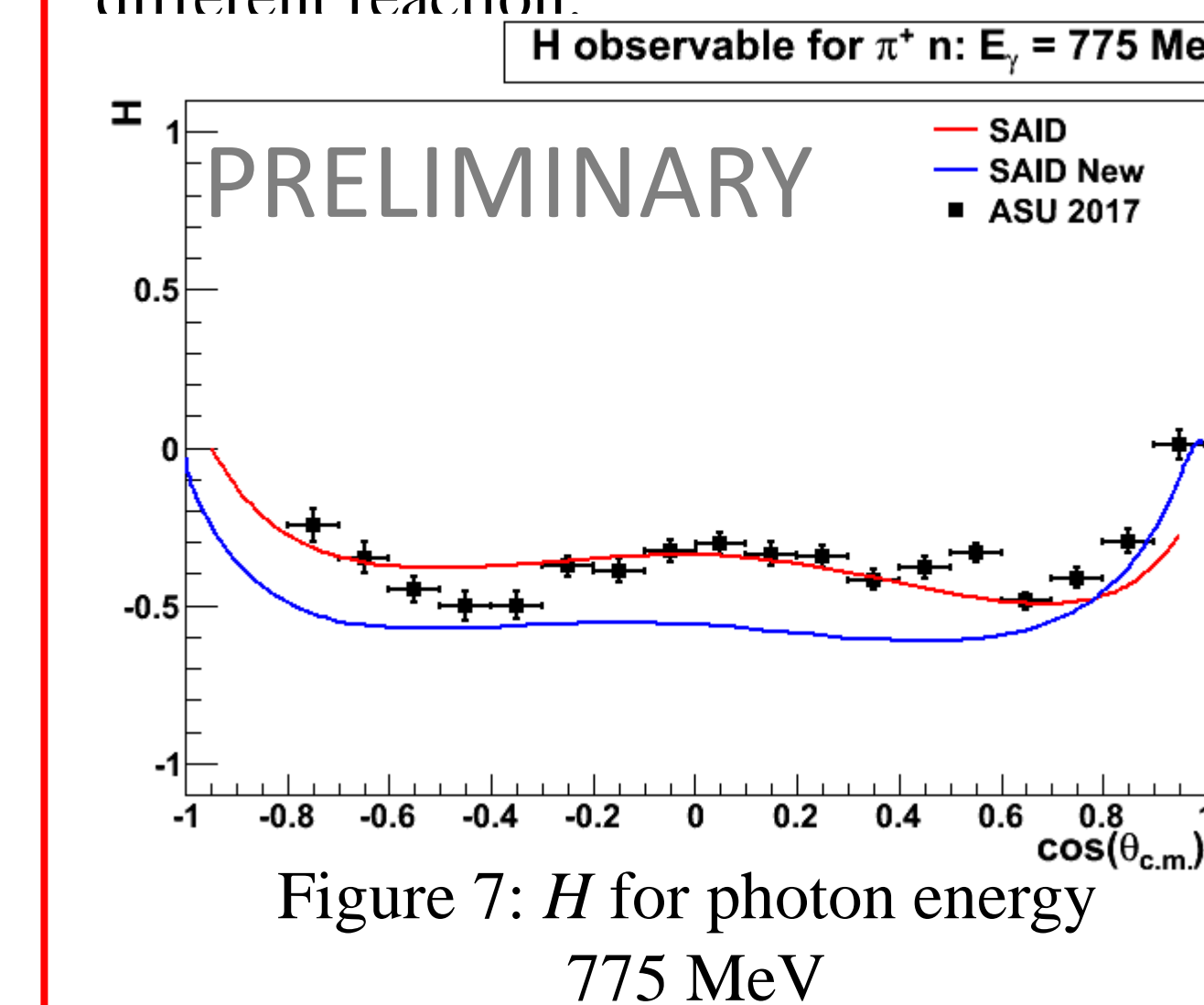


Figure 7: H for photon energy 775 MeV

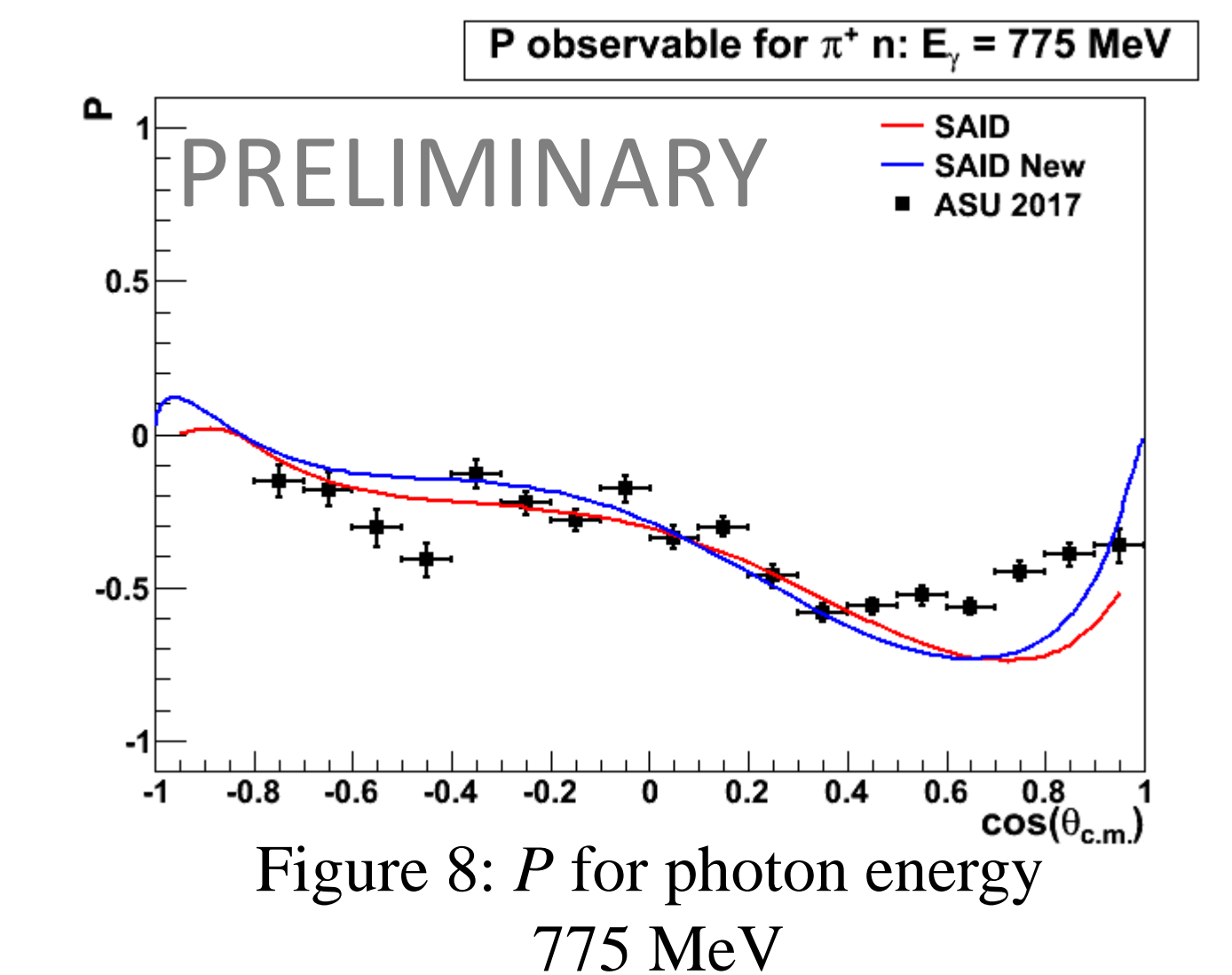


Figure 8: P for photon energy 775 MeV

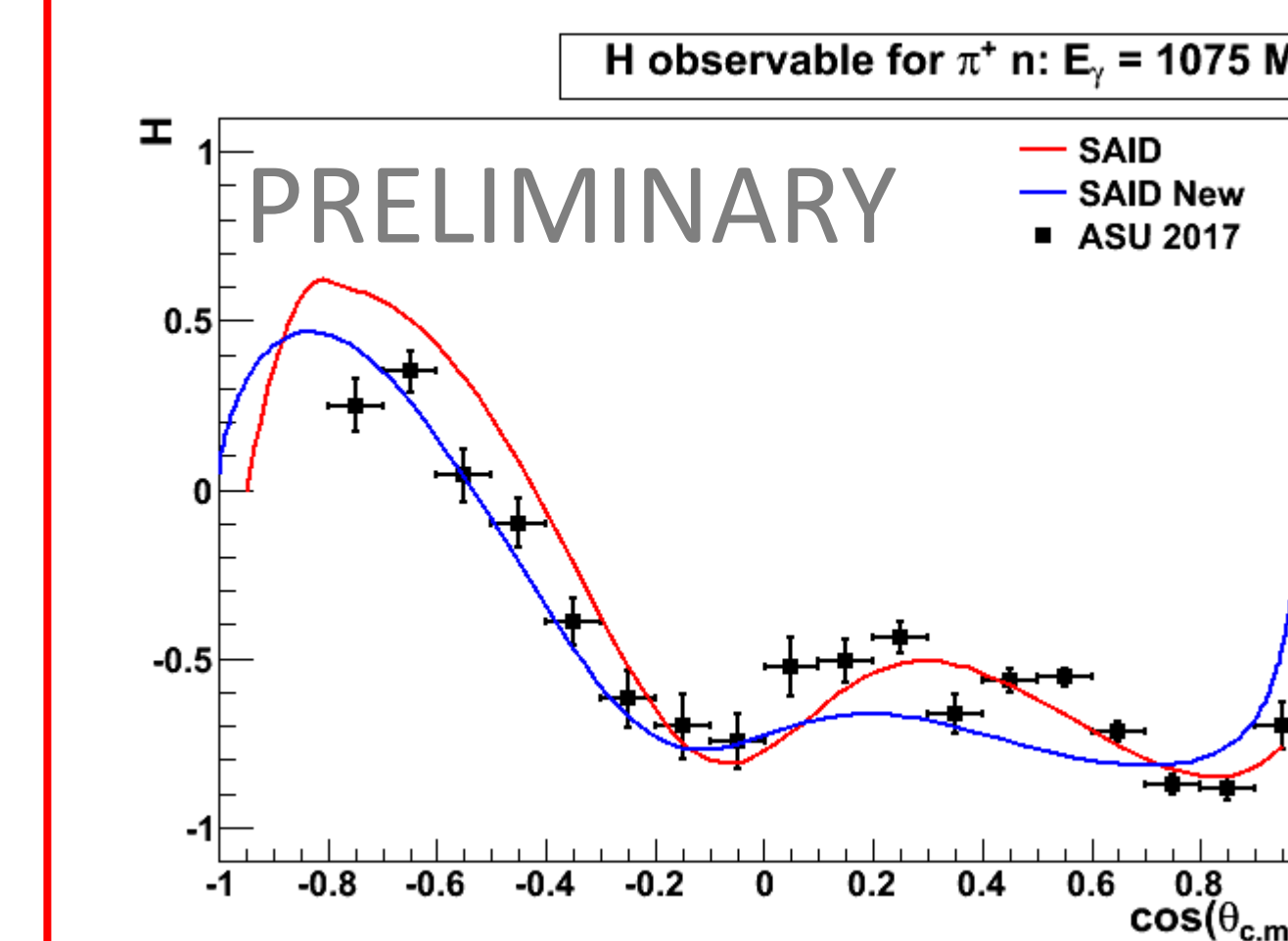


Figure 9: H for photon energy 1075 MeV

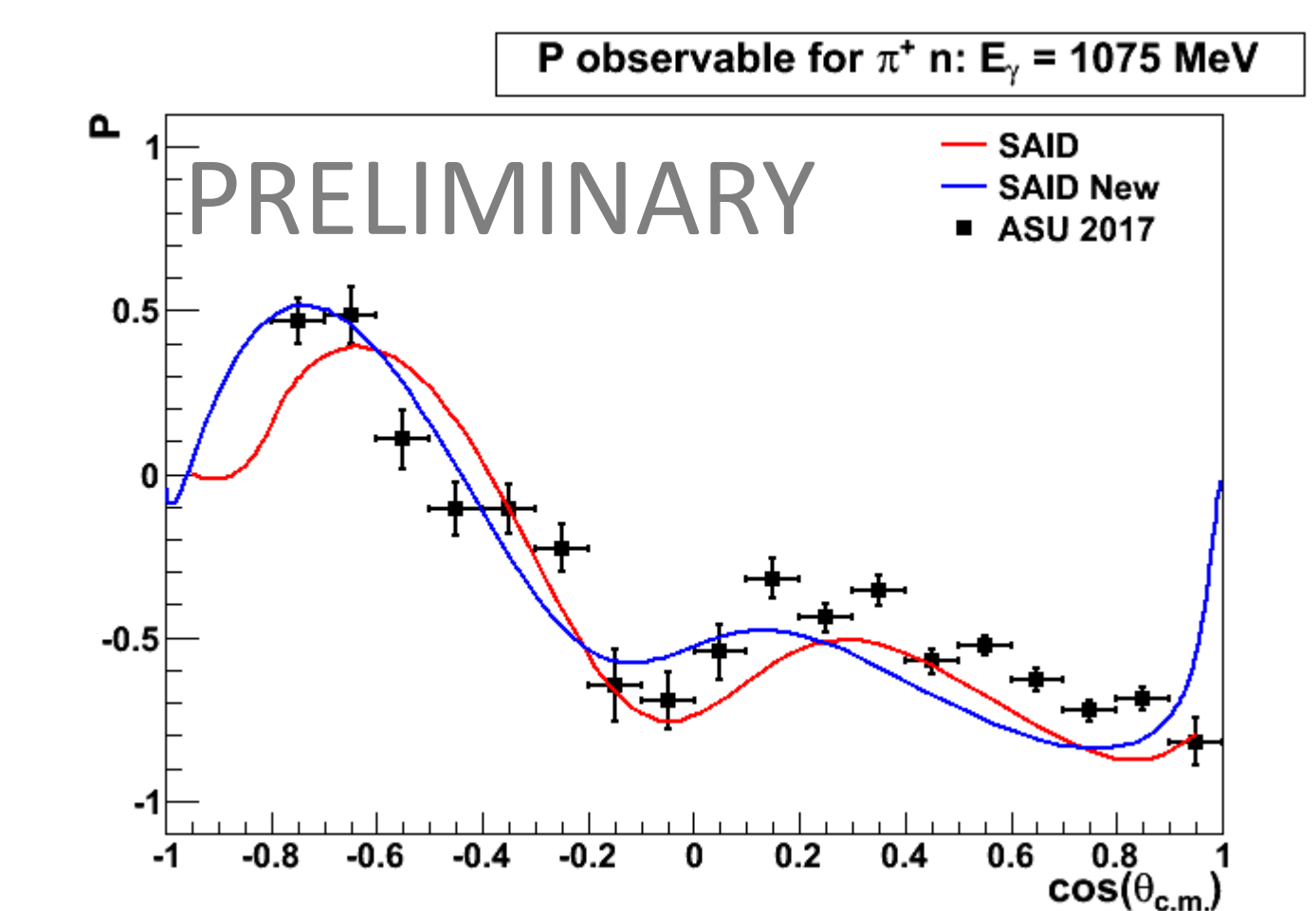


Figure 10: P for photon energy 1075 MeV

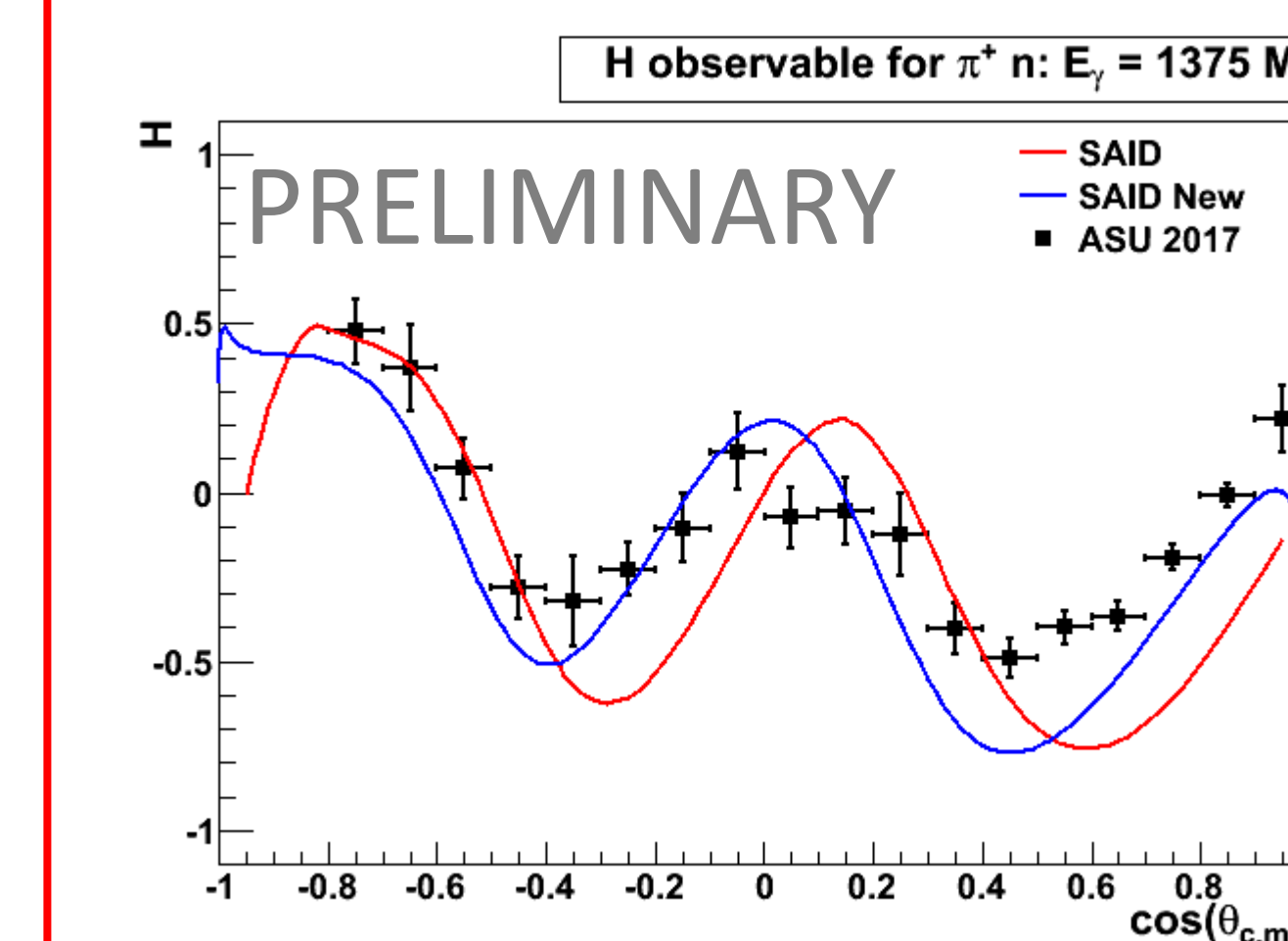


Figure 11: H for photon energy 1375 MeV

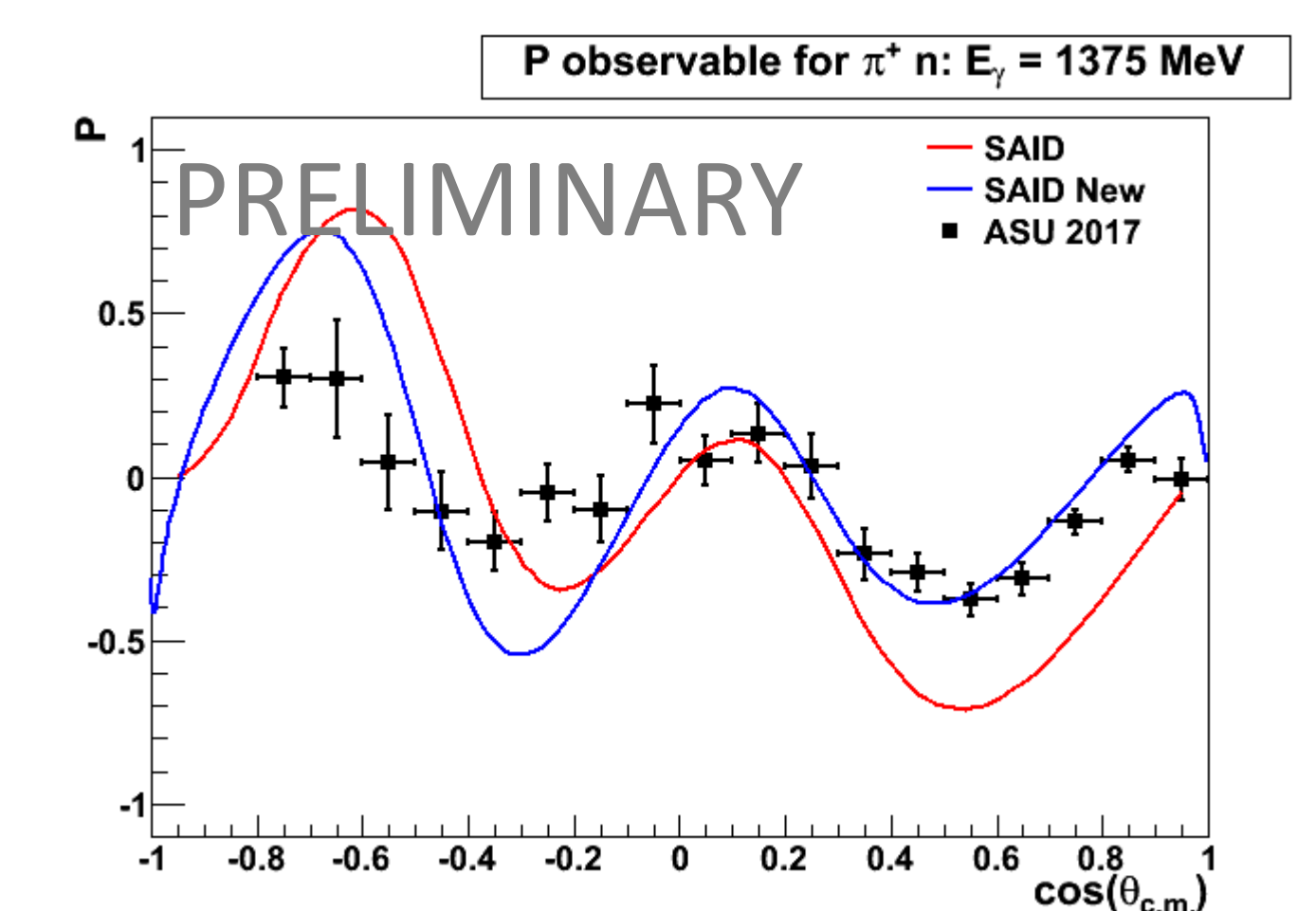


Figure 12: P for photon energy 1375 MeV

Conclusions

As can be seen, the values obtained for H and P compare well to the theoretical predictions from the SAID Partial Wave Analysis Facility. Importantly, however, there exists no published data in this energy range for this specific reaction. As a result, these values for H and P can be used to constrain future PWA predictions.

From our data, a better understanding of nucleon resonances can be obtained, which further allows for the disentanglement of the various resonances of the nucleon. These results, then, are a step towards further understanding the nature of the nucleons, the fundamental building-blocks of all matter.